Aerodynamic Characteristics Improving of S809 Airfoil in Wind Turbine with Microtab

Ressan Faris Al-Maliky
Engineering College, University of Kufa/ Al-Najaf
Emil: uot_magaz@yahoo.com

Abstract:
In present work numerical two dimensions, steady, incompressible, turbulent flow past S809 wind turbine airfoil with microtab at 95% of chord length of leading edge in lower surface is analyzed by Fluent (6.2) program for model consists of S809 airfoil without and with microtab at 95% of chord line have height 1.1% and other 2% of chord length undergo to turbulent flow k-ε model, the flow has Reynolds number is 10^6. The results are represented by velocity contour and vector. Aerodynamic coefficients are drawn in graph. The results are showed an increase lift and drag coefficient in existence microtab locate 95% of chord at it's height 1.1% and 2% of chord to range of attack angle (0, 5, 10, 15, 20) degrees. The results compare with experimental data of standard airfoil and existence 1.1% chord length microtab and it is approximately good. Values of lift & drag coefficient are increased for the existence of 1.1% chord length microtab while in case the existence of microtab 2% chord length lift coefficient increased which it's max. increment by 46% while, drag coefficient decreased it's min. increment to be 26% but not full range of attack angle.

Keywords: S809, k-ε turbulent, Microtab.

تحسين الخواص الايروديناميكية لريشة نوع S809 في توربين هوائي باستخدام جنيح

الخلاصــة

في هـذا الموضـوع دراسـة عدديـة لجريـان ثنـائي الإبعـاد , مستقر ، غيـر انضـغاطي مضطرب نوع k-ε حول ريشة نوع S809 لتوربين هوائي مع جنيح موضوع علـى بعد 95٪ طول الريشة من مقدمة الريشة لسطح السفلي. التحليل تم بواسطة برنـامج (6.2) Fluent لنمـوذج الريشة بدون وبوجود الجنيح بطـول 1.1٪ والحالـة الأخرى بــ 2٪ طـول الريشـة لمدى من زوايـا الهجوم (0 , 5 , 10 , 15 , 20) درجة ورقم رينولدز يساوي 10^6 .

النتائج مثّلت كخرائط كنتورية لسرعة ودقائق الجريان. المعاملات الآيروديناميكية رسمت بشكل مخططات بيانية وتم مقارنتها مع نتائج تجريبية لباحثين أخريين لنموذج الريشـة فقط وكذلك بوجود الجنيح بطول 1.1٪ طول الريشـة لمعامل الرفع وكانت نتائج المقارنـة جيدة تقريبـاً , كمـا بينت زيادة معاملي الرفع والكبح عندما كان طول الجنيح 1.1٪ طـول الريشـة كذلك زيادة معامل الرفع بحيث الزيادة في قيمته العظمى 46% بينما معامل الكبح يقل وبنقصـان فـي قيمتـه الصـغرى 26% ولكن ليس على طول مدى زاوية الهجوم في حـلـة طول الجنيح يساوي 2٪ طول الريشة .

Nomenclature:

Latin symbols	Description
a_1, a_2	coordinate transformation coefficients
C	chord length (m)
J	jacobean of transform matrix for the curvilinear coordinate system
k	turbulent kinetic energy (m^2/s^2)
U_∞	free air velocity (m/s)
G_1, G_2	contravariant velocity component in x, y – direction respectively
P	local pressure (N/m^2)
C_p	pressure coefficient
C_f	skin friction coefficient
C_N	normal force coefficient
C_A	axial force coefficient
$S_{(Mx, My, k, \varepsilon)}$	source term due to non-orthogonal characteristic of grid system
C_d	drag coefficient
N	normal force (N)
A	axial force (N)
C_l	lift coefficient
U_∞	free velocity of air (m/s)
$(L/D)_{max}$	Lift to drag maximum ratio
u, v	velocity component in x, y – direction respectively (m/s)
x	cartesian coordinate in horizontal direction (m)
y	cartesian coordinate in vertical direction (m)

Greek symbols	Description
τ	shear stress (N/m^2)
α	angle of attack (degree)
ε	dissipation of turbulent kinetic energy (m^2/s^2)
ρ	density of the air (kg/m^3)
ξ, η	dimensionless body-fitted coordinates
$\Gamma_{(u, v, k, \varepsilon)}$	diffusion vector
μ_{eff}	dynamic viscosity of the air (kg/m.s)

symbols	Abbreviations
CFD	Computational Fluid Dynamic
S809	NREL's S-Series Wind Turbine Airfoil have 21%C maximum thickness
NREL	National Renewable Energy Laboratory
tab1	Airfoil with microtab locate 95%C from leading edge with height 1.1%C
tab2	Airfoil with microtab locate 95%C from leading edge with height 2%C

INTRODUCTION

Improving performance of wind turbine airfoil by using microtabs as a device for active load control applications is located close to the trailing edge like to Gurney flap or flap itself. Microtabs are perpendicular to lower surface of airfoil approximately where incline with small angle with chord line. In fact aerodynamic forces exerted on tab are analyzed to lift and drag in additional to lift of airfoil at high speed drag force given separation in boundary layer at front of tab therefore, using it in wind turbine due to low speed reach in the present to 14.61 m/sec [5].

Peter Baek & Mac Gaunaa (2001) analyzed the temporal response of the microtab, they show that it has two disadvantages compared with a trailing edge flap, when considering it for active load control of a wind turbine. First of all the microtab has a reverse control phenomenon in initial phase of deployment, and second of all the response is delayed, compared with the flap, due to buildup of flow structures. To find an engineering model for the temporal response of the microtab to investigate the behavior of the microtab in an aeroelastic model of a wind turbine. Before they attempted to model the microtab in detail, they inserted temporal of the microtab found with CFD directly into the aeroelastic code FLEX5. They found that the reverse control was not important for the response of the blade. They propose to use a simple queue delay to model the flow physics of the microtab. They calculated the load reduction potential of the microtab, assuming that they could model it as a delay, and compared it to that of a trailing edge flap. In them calculation the trailing edge flap had a load reduction potential twice as big as the microtab solution [1].

Raymond Chow & C. P. van Dam (2007) analyzed flow about a wind turbine airfoil with a deploying microtab device has been numerically simulated by solving unsteady turbulent compressible two-dimensional, Navier-Stokes equations with the OVERFLOW2 solver. Using a Chimera/overset grid topology, microtabs were placed at 95% of chord of a S809 airfoil. Microtab heights on the order of 1% of chord, deployed on the order of one (1) characteristic time unit were utilized. The effect of free stream angle of attack on the aerodynamic response was also investigated. Validation studies with experimental results for static deployed microtabs and a dynamically deployed spoiler were also performed to ensure accurate temporal and spatial resolution of the numerical simulations [2].

C.P. Van Dam et al (2007) reduced the cost of wind-generated electricity by mitigating fatigue loads acting on the blades of wind turbine rotors. One way to accomplish this is with active aerodynamic load control devices that supplement the load control obtainable with current full-span pitch control. Techniques to actively mitigate blade loads that are being considered include individual blade pitch control, trailing-edge flaps, and other much smaller trailing-edge devices such as microtabs and microflaps. The focus of their work is on the latter aerodynamic devices, their time-dependent effect on sectional lift, drag, and pitching moment, and their effectiveness in mitigating high frequency loads on the wind turbine [3].

J.J. Wanga et al (2007) have been used the Gurney flap Since its invention by a race car driver Dan Gurney in 1960s, it used to enhance the aerodynamics performance of subsonic and supercritical airfoils, high-lift devices and delta wings. In order to take stock of recent research and development of Gurney flap, they have carried out a review of the characteristics and mechanisms

of lift enhancement by the Gurney flap and its applications. Optimum design of the Gurney flap is also summarized in them paper. For the Gurney flap to be effective, it should be mounted at the trailing edge perpendicular to the chord line of airfoil. The flap height must be of the order of local boundary layer thickness. For subsonic airfoils, an additional Gurney flap increases the pressure on the upstream surface of the Gurney flap, which increases the total pressure of the lower surface. At the same time, a long wake downstream of the flap containing a pair of counter rotating vortices can delay or eliminate the flow separation near the trailing edge on the upper surface. Correspondingly, the total suction on the airfoil is increased. For supercritical airfoils, the lift enhancement of the Gurney flap mainly comes from its ability to shift the shock on the upper surface in the downstream. Applications of the Gurney flap to modern aircraft design are also discussed in this review [4].

Baker et al (2005) conducted more comprehensive 2-D computational experiments further examining tab height and location on both upper and lower surface on the S809 and the GU25-5(11)8 airfoil. Pressure surface tabs demonstrated increase lift over all angles of attack, whereas suction surface tabs only decrease lift at angles of attack throughout the linear region. The suction surface tabs loses effectiveness at the higher angles of attack because the flow separates forward of the tab location. The optimal location for the lower surface tab in terms of lift and drag was again found to be around $95\% c$ with a height on the order of the boundary layer thickness, or $\sim 1\% c$. The computational studies were validated in the wind tunnel on the S809 airfoil [6].

MATHEMATICAL FORMULATION:

Consider steady, two dimensional, turbulent k-ε model, and incompressible flow over S809 airfoil with microtab as shown in Fig. (1). The differential equations that describe the flow were integrated by the finite volumes method in two dimensions by FLUENT software package.

Continuity and Navier – Stokes or momentum equations are the governing equations for the problem are analyzed in a two – dimensional incompressible flow steady, fully viscous subsonic flow of a Newtonian fluid, continuity and momentum equation become, respectively [7]:

continuity equation:

$$\frac{\partial u}{\partial x} + \frac{\partial v}{\partial y} = 0 \qquad \qquad ....(1)$$

In x - direction (*u*-momentum):

$$r\left(u\,\frac{\partial u}{\partial x} + v\,\frac{\partial u}{\partial y} \right) = \frac{\partial P}{\partial x} + \frac{\partial}{\partial x}\left(2m_{eff}\,\frac{\partial u}{\partial x} \right) + \frac{\partial}{\partial y}\left(m_{eff}\,\frac{\partial u}{\partial y} \right) + \frac{\partial}{\partial y}\left(m_{eff}\,\frac{\partial v}{\partial x} \right) \ ... \ (2)$$

In y - direction (*v*-momentum):

$$r\left(u\,\frac{\partial v}{\partial x} + v\,\frac{\partial v}{\partial y} \right) = \frac{\partial P}{\partial y} + \frac{\partial}{\partial x}\left(m_{eff}\,\frac{\partial v}{\partial x} \right) + \frac{\partial}{\partial y}\left(2m_{eff}\,\frac{\partial v}{\partial y} \right) + \frac{\partial}{\partial x}\left(m_{eff}\,\frac{\partial u}{\partial y} \right) ... \quad (3)$$

x – momentum:

$$\frac{\partial}{\partial x}\left(rG_1 u\right)+\frac{\partial}{\partial h}\left(rG_2 u\right)=\frac{\partial}{\partial x}\left(\Gamma_u Ja_1 \frac{\partial u}{\partial x}\right)+\frac{\partial}{\partial h}\left(\Gamma_u Ja_2 \frac{\partial u}{\partial h}\right)+S_{MX} \qquad \dots (4)$$

y – momentum:

$$\frac{\partial}{\partial x}\left(rG_1 v\right)+\frac{\partial}{\partial h}\left(rG_2 v\right)=\frac{\partial}{\partial x}\left(\Gamma_v Ja_1 \frac{\partial v}{\partial x}\right)+\frac{\partial}{\partial h}\left(\Gamma_v Ja_2 \frac{\partial v}{\partial h}\right)+S_{MY} \qquad \dots (5)$$

k – equation:

$$\frac{\partial}{\partial x}\left(rG_1 k\right)+\frac{\partial}{\partial h}\left(rG_2 k\right)=\frac{\partial}{\partial x}\left(\Gamma_k Ja_1 \frac{\partial k}{\partial x}\right)+\frac{\partial}{\partial h}\left(\Gamma_k Ja_2 \frac{\partial k}{\partial h}\right)+S_k \qquad \dots (6)$$

ε – equation:

$$\frac{\partial}{\partial x}\left(rG_1 e\right)+\frac{\partial}{\partial h}\left(rG_2 e\right)=\frac{\partial}{\partial x}\left(\Gamma_e Ja_1 \frac{\partial e}{\partial x}\right)+\frac{\partial}{\partial h}\left(\Gamma_e Ja_2 \frac{\partial e}{\partial h}\right)+S_e \qquad \dots (7)$$

S809 Airfoil Section

The airfoil of interest for this study is the 21-percent thick S809; an airfoil from the NREL thick-airfoil family airfoil for horizontal-axis wind-turbine applications. For this purpose the airfoil was designed to have a sustained maximum lift, minimal sensitivity of lift to roughness, and low profile drag [9] as Figure (1).

AERODYNAMIC CHARACTERISTICS:

Application of momentum conservation laws show that the forces and moments on an airfoil due to two sources once pressure distribution on the surface of the airfoil, and other shear stress distribution over the surface of the airfoil [9].

The pressure forces act normal to the surface of the airfoil and the shear stress acts tangential to the surface of the airfoil the integration of these two distributions over the surface of the airfoil yields a resultant force and moment. This resultant force can be divided into two components: one perpendicular to the chord line, the normal force (N) and other parallel to the chord line, the axial force (A) as Fig. (15). The pressure coefficient and the shear stress coefficients are given as[8]:

$$C_p = \frac{P - P_\infty}{\frac{1}{2} rU_\infty^2} \qquad \dots (16)$$

$$C_f = \frac{t}{\frac{1}{2} rU_\infty^2} \qquad \dots (17)$$

So, the lift coefficient and drag coefficient are related by:

$$C_l = C_N \cos a - C_A \sin a \qquad \dots (18)$$

$$C_d = C_N \sin a + C_A \cos a \qquad \dots (19)$$

Grid Generation:

   Grid is generated by using GAMBIT in which geometry is drawn then divided
to mesh is exported to FLUENT. The numerical calculations are done in it for
varying angle of attack to purpose of estimate aerodynamics coefficients.

   The grid microstructure is created in GAMBIT and is divided into non-uniform
quadrilateral cells or elements having a total 61,474 and 33,705 nodes around
airfoil only, but it's with microtab has quadrilateral & triangle elements are 76,678
and 41,281 nodes.

   Convergences at every step are checked and it's value of (10^6) in about 3000
iterations in each case.

RESULTS AND DISCUSSION:

   The numerical results are represented for S809 airfoil has chord line length 1
m, 21%C maximum thickness with microtab locate at 95%C of leading edge which
has been taken two cases first has length 1.1%C and other 2%C as shown in Figs.
(2, 4). Reynolds number equal 10^6, 1% turbulence intensity and 0.01 turbulent
length scale by contour or flow map. The airfoil without & with microtab 1.1%C &
2%C cases are represented aerodynamic coefficients with range of angles of attack
are (0, 5, 10, 15, 20) degrees using Fluent (6.2) program by vectors and contours
velocity in additional to graphs.

   Vectors and contours velocity airfoil with microtab and height 1.1%C in Figs.
(2, 3): show distribution of air particle around airfoil and microtab appear
circulation flow in rear side of microtab of airfoil this circulation flow will increase
as angle of attack increasing until 20 degrees in this time separation in boundary
layer flow is fully complete from leading to trailing edge of airfoil in other words
separation is existence before 20° attack angle appear over upper surface and then
connect separation of upper with lower surface at rear side of microtab as Fig. (3).

   Figures. (4, 5, 6, and 7): show flow past airfoil with microtab locate 95%C and
height 2%C, circulation and separation in boundary layer appear in rear side of
microtab further than that has height 1.1%C due to long microtab, therefore,
separation will increase when angle of attack increases from 0, 5, 10 until 15
degrees happen connect between separation in upper and lower (rear side of
microtab) surface shows in Fig. (7).

   The results of lift coefficient of S809 airfoil without and with microtab have
heighted 1.1%C are compared with experimental data for other researcher (Baker
et al, 2005) as shown in Figs. (8, 9). Numerical lift coefficient greater than it's
experimental values in Fig. (8). this increment will increase as angle of attack
increases that this comparison gives a good approach for lift coefficient.

   Figures. (9): comparison numerical and experimental of S809 airfoil with
microtab locate at 95% with 1.1%C length, note that experimental greater values
than numerical but at 17.5 degrees angle of attack begin as experimental values
across with other. Its values will decrease as angle of attack increases in small
period because surface roughness, or perhaps data accuracy and humidity of air of
experiment results in which take pure in FLUENT results.

   Comparison between lift coefficient without and with microtab 95%C from
leading edge and it's length of 1.1%C is numerically shown in Fig. (10). This
increases lift coefficient with microtab further from standard airfoil lift values as
increase in attack angle but at 12 degrees angle of attack where cross with other

curve then decrease in it's values, while note Fig. (11): represents different between experimental without and with microtab, clearly lift coefficient with microtab is more than that no microtab along range of angle of attack.

In relative to drag coefficient must be known effect after insert microtab where Fig. (12): numerical values of drag coefficient verse angle of attack, is clearly found increment in drag coefficient of airfoil with microtab than standard it due to circulation or eddy in rear side of microtab where this circulation work on decreasing back pressure of airfoil.

In case of increasing in height of microtab to 2%C, as shown in Figs. (13, 14), of relation between aerodynamic coefficient and angle of attack of S809 airfoil with two cases of microtab height 1.1%C & 2%C (called tab1 & tab2 respectively in figures) in addition to standard airfoil.

In Fig. (13): there are increments in lift coefficient values that have 2%C height than other that have 1.1%C height microtab until cross with 1.1%C at 14 degrees angle of attack then reduces to cross with standard airfoil at 17.5° angle until 20° degrees attack angle its value is lower than two other cases due to incline surface of microtab in zero attack angle will increase to work right angle or further to normal angle with flow; therefore, become microtab like to baffle plate generate lift force with opposite direction i.e., down direction works to reduce lift coefficient.

While in Fig. (14): shows decreasing drag coefficient of airfoil has 2%C height microtab is clearly further than two other cases until 13° attack angle and then will increase further to 20 i.e., range 0° to 13° is advantage limit, but after 13° attack angle microtab becomes normal on line of flow or flow velocity; therefore, its form resistance has opposite motion of airfoil.

In Fig. (16): is represented relationship between C_l & C_d it's behavior remains relatively constant until the airfoil reaches maximum lift coefficient then the drag coefficient begins in increase dramatically with small decreasing to lift coefficient in each cases (with and without microtab). To find the best glide ratio, have to draw a line from the origin tangentially to the curve, the values of C_l & C_d at the point where the line touches the curve which C_l / C_d ratio represent glide ratio and it is maximum value same as $(L/D)_{max}$ to be 11.0769 for the standard airfoil another $(L/D)_{max} = 32.8$ for airfoil with microtab has 2%C height at range $(5 − 10)$ degrees attack angle in each case.

CONCLUSIONS

1. The lift coefficient values of airfoil with height 1.1%C at 95%C from leads to edge greater than it's values without microtab as the attack angle increases until the angle 12 degrees.
2. Increasing the lift coefficient of airfoil has microtab and its height 2%C is further than its values existence of 1.1%C microtab has the same location, also further than standard airfoil until the angle 14 degrees after this decreasing further than two another cases.
3. The drag coefficient values of airfoil with microtab height 1.1%C higher than it's values without microtab in full range of attack angle i.e., (0 to 20) degrees.
4. The drag coefficient values of airfoil with microtab have 2%C height is decreased more than it's values in standard airfoil and with microtab have

3259

1.1%C height with angle of attack until the angle 13 degrees, begin increases and continuous increasing until it reaches to 20 degrees.

REFERENCES

[1] Baek, Peter; Gaunaa, Mac. "Modeling the Temporal Response of a Microtab in an Aeroelastic Model of a wind Turbine". AIAA journal, Denmark, 2001.

[2]Chow, Raymond; Van Dam, C. P. "Computational Investigations of Deploying Load Control Microtabs on a Wind Turbine Airfoil". AIAA – 2007 – 1018, PP. 14, 2007.

[3]Van Dam, C. P.; Chow, R.; Zayas, J.R.; Berg, D.E. "Computational Investigations of Small Deploying Tabs and Flaps for Aerodynamic Load Control". The Science of Making Torque from Wind J. of Physics, IOP Publishing, 2007.

[4]Wanga, J. J.; Li Y.C.; Choi, K. S. "Gurney Flap—Lift Enhancement, Mechanisms and Applications". Elsevier J., November 2007.

[5]Johnson, Scott J.; Van Dam, C. P. Case; Berg, Dale E. "Active Load Control Techniques for Wind Turbines". SANDIA Report, SAND2008-4809, Sandia National Laboratories, Albuquerque, New Mexico 87185 & Livermore, California 94550, August 2008.

[6]Baker, J. P.; Standish, K. J.; Van Dam, C. P. "Two-Dimensional Wind Tunnel and Computational Investigation of a Microtab Modified S809 Airfoil". AIAA Paper 2005-1186, 43rd AIAA Aerospace Sciences Meeting and Exhibit, Reno, NV, 2005.

[7]Ahmed, S. Sh. "Modeling of Attached and Detached Turbulent Viscous Flow over Symmetrical Aerofoil". M. Sc. Thesis, University of Babylon, 2009.

[8]Al-Jibory, M. W. "The Effect of Internal Acoustic Excitation on the Aerodynamic Characteristics of Airfoil". Ph. D., Thesis, University of Technology, 2007.

[9]Sommers, D. M.. "Design and Experimental Results for the S809 Airfoil" NREL/SR-440-6918, January 1997.

[10]National Wind Technology Center (coordinate of S809) http://wind.nrel.gov/airfoils/Shapes/S809_Shape.html
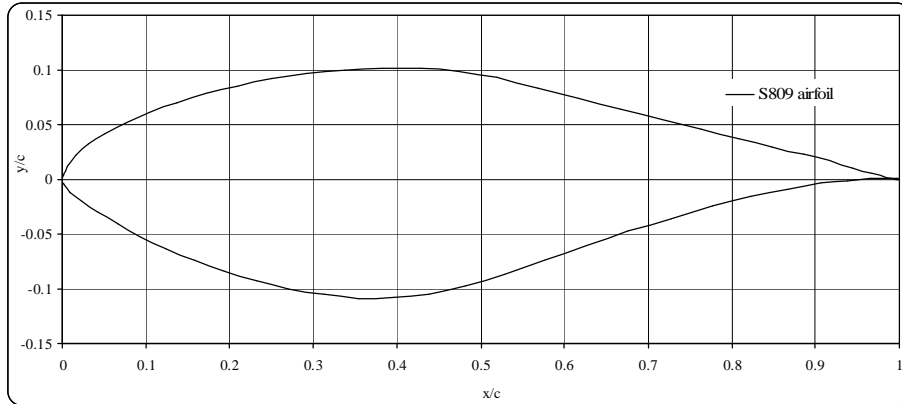
Figure(1) Coordinate of S809 profile airfoil.
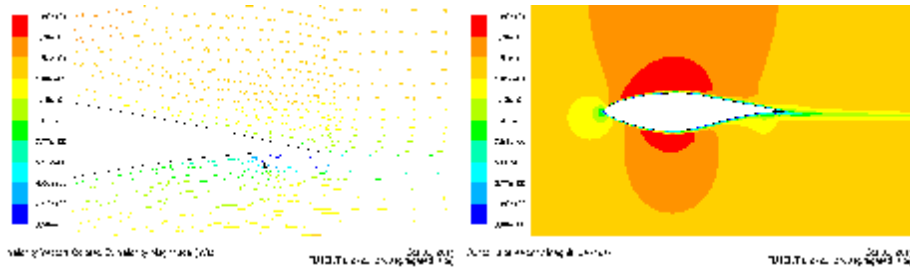
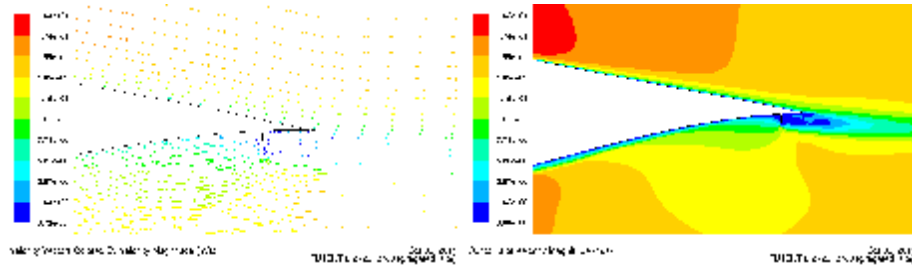**Figure(2) Airfoil with microtab with height 1.1%C at zero angle of attack.**
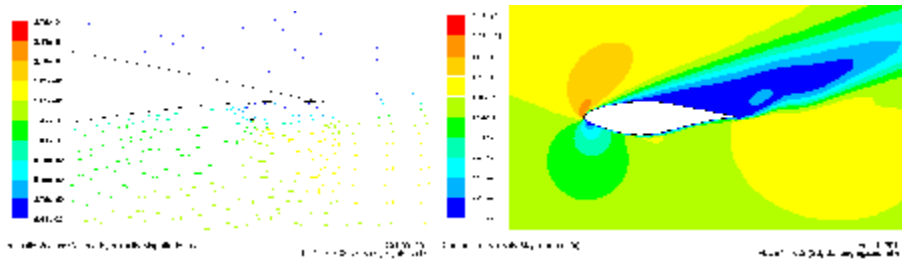
Figure (3) Airfoil with mircotab with height 1.1%C at 20 angle of attack.

3261

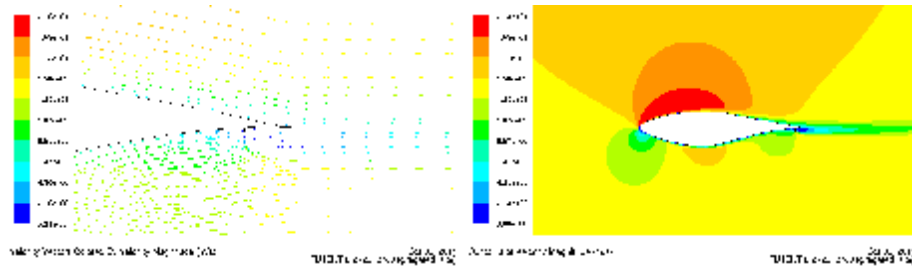**Figure(4) Airfoil with microtab with height 2%C at zero angle of attack.**

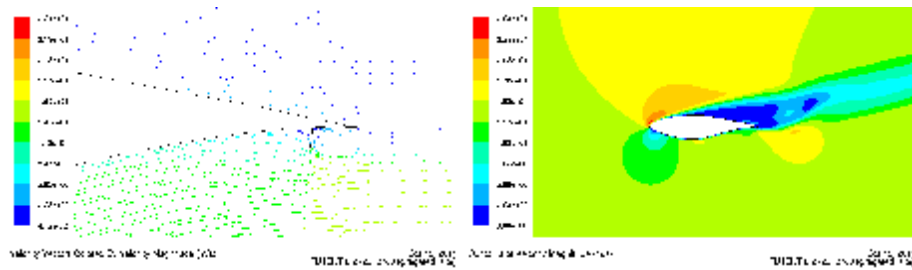**Figure (5) Airfoil with microtab with height 2%C at 5 angle of attack.**

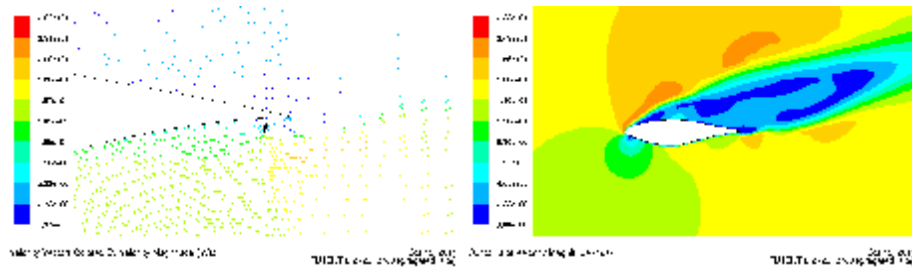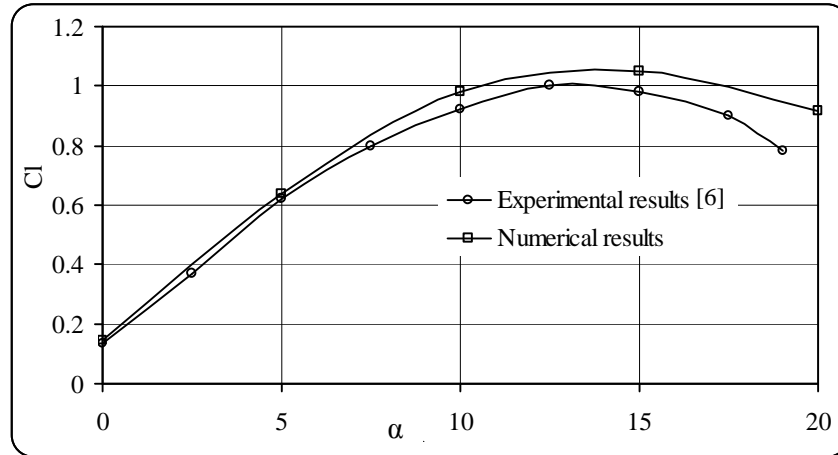**Figure (6) Airfoil with microtab with height 2%C at 15 angle of attack.**

Figure (7) Airfoil with microtab with height 2%C at 20 angle of attack.

Figure (8) Comparison between experimental and numerical lift coefficient of S809 standard airfoil lift coefficient vs. angle of attack.
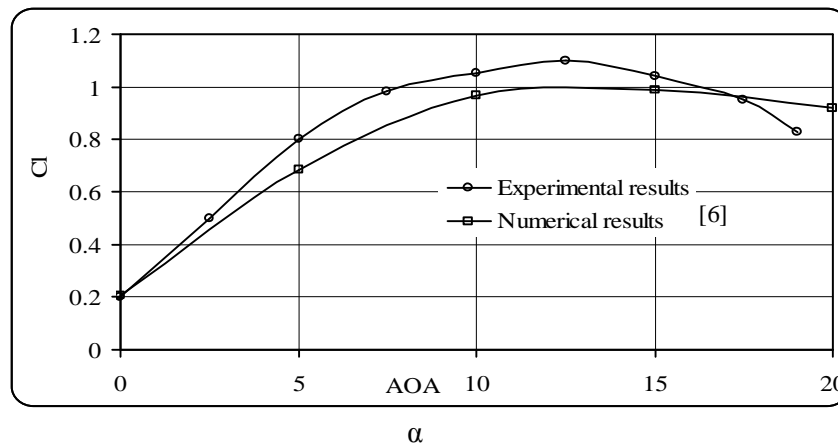
Figure (9) Comparison between experimental and numerical lift coefficient of S809 airfoil with microtab with height 1.1%C vs. angle of attack.
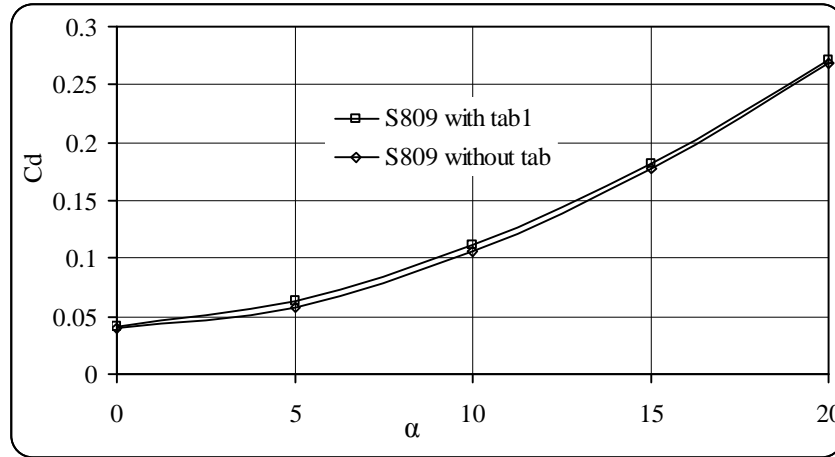
3263
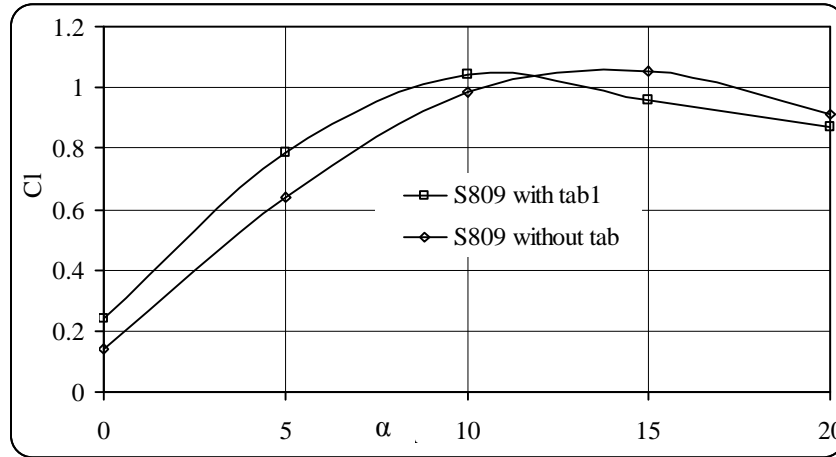
Figure (10) Comparison between numerical lift coefficient of S809 airfoil without and with microtab locate 95%C from leading edge with height 1.1%C vs. angle of attack.
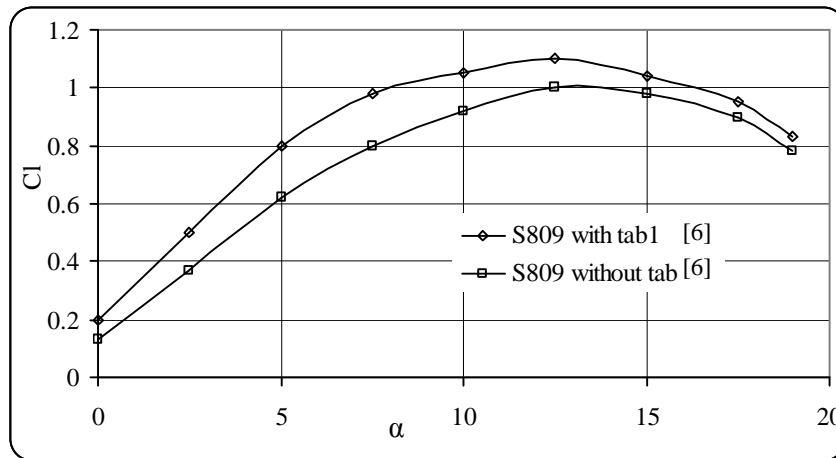
Figure (11) Comparison between experimental lift coefficient of S809 airfoil without and with microtab with height 1.1%C vs. angle of attack.
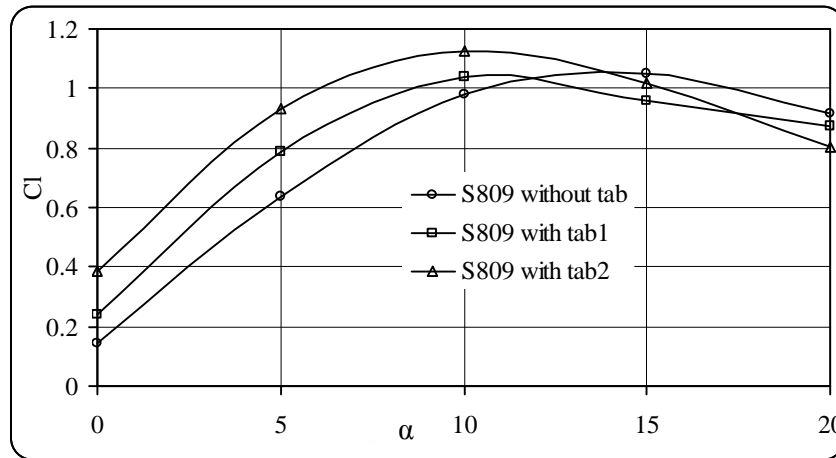
3264

Figure (12) Comparison between numerical drag coefficient of S809 airfoil without and with microtab with height 1.1%C vs. angle of attack.

Figure (13) Comparison between numerical lift coefficient of S809 airfoil without and with microtab with height 1.1%C and another 2%C vs. angle of attack.
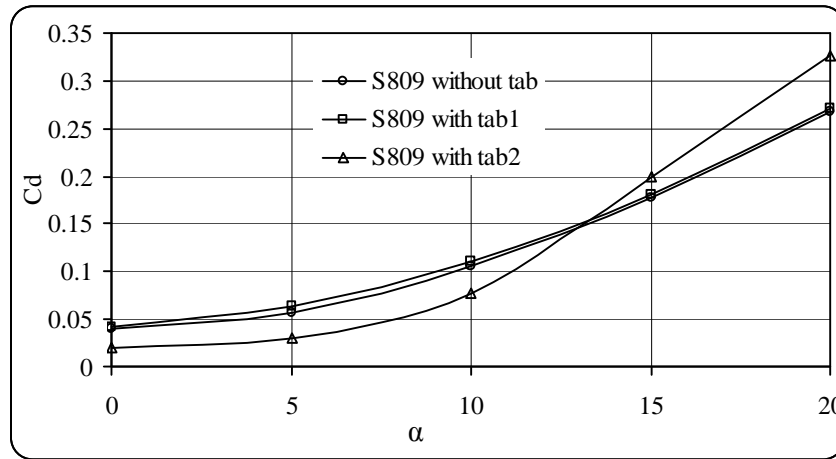
3265

Figure (14) Comparison between numerical drag coefficient of S809 airfoil without and with microtab with height 1.1%C and another 2%C vs. angle of attack.
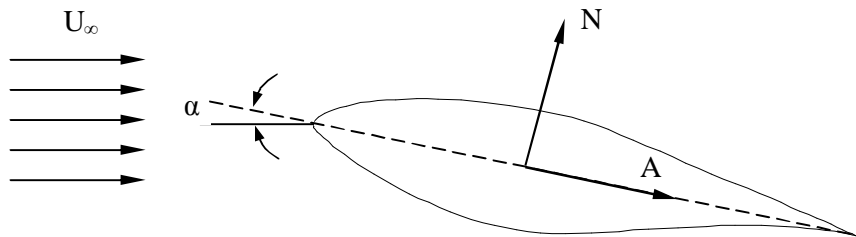

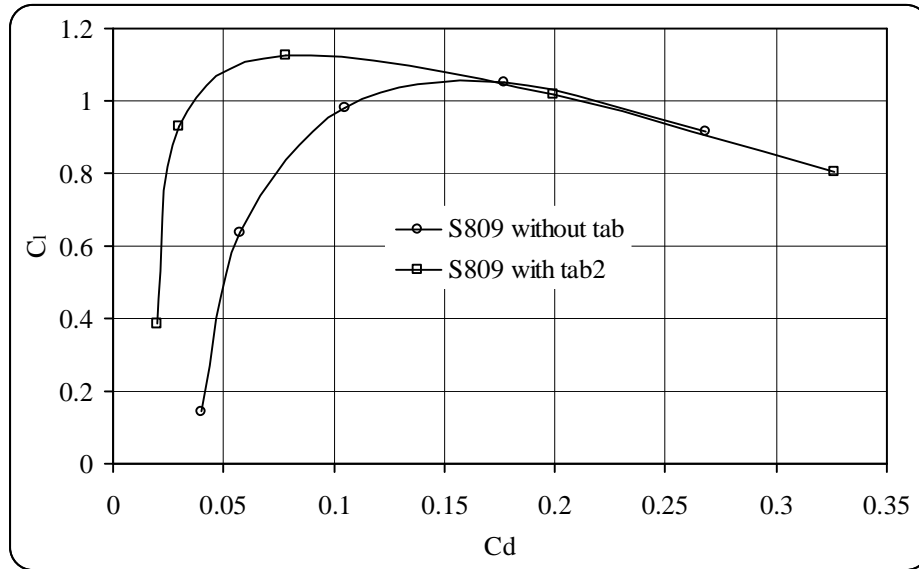**Figure (15) Components of the aerodynamics forces on airfoil**

Figure (16) Numerical of airfoil S809 without & with microtab has 2%C height.